THESIS FOR THE DEGREE OF LICENTIATE OF ENGINEERING

Speciation of copper in ashes from municipal solid waste combustion

HENRIC LASSESSON

Department of Chemical and Biological Engineering
Industrial Materials Recycling

CHALMERS UNIVERSITY OF TECHNOLOGY

Gothenburg, Sweden 2013

Speciation of copper in ashes from municipal solid waste combustion
HENRIC LASSESSON

Technical report no 2013:13
ISSN: 1652-943X

Industrial Materials Recycling
Department of Chemical and Biological Engineering
Chalmers University of Technology
SE-412 96 Gothenburg
Sweden
Telephone + 46 (0)31-772 1000

Cover:
The experimental hall at beamline I811 of the MAX II synchrotron, Lund, Sweden, where all x-ray absorption spectroscopy measurements used in this thesis has been conducted.

Chalmers Reproservice
Gothenburg, Sweden 2013

Speciation of copper in ashes from municipal solid waste combustion

HENRIC LASSESSON

Industrial Materials Recycling
Department of Chemical and Biological Engineering
Chalmers University of Technology

Abstract

Copper is one of the most important trace elements in municipal solid waste (MSW) combustion. Knowledge of the speciation of copper is fundamental for the understanding of the effects of copper compounds on the combustion chemistry as well as of the environmental impact of the ash. An increased understanding of the chemistry of copper in combustion and in the ashes could support the development of management and recycling techniques, not only for the copper metal but also for the bulk of the ash. It could also increase the understanding of how it might be possible to reduce the amount of dioxins formed and thereby reducing the toxicity of the ashes as well as the flue gases. In this work the speciation of copper in four ash flows from a bubbling fluidized bed (BFB) boiler and one fly ash from a grate fired mass burn (MB) combustor has been investigated using synchrotron based X-ray absorption spectrometry. Additionally the copper speciation of leaching residues from the BFB filter ash and MB fly ash, leached in ammonium nitrate and nitric acid, have also been investigated. The results from the BFB ash flows showed that copper occurred mainly as copper metal, copper oxides and mixed oxides in the ashes from and close to the combustion bed. The concentrations of copper sulphate, hydroxides and chlorides increased further down the BFB flue gas system, closer to the filter. Copper in oxidation states 0, +I and +II was found in all ash flows, except in the BFB filter ash where mainly copper(II) was found. The MB fly ash showed significantly different copper speciation than in the BFB fly ash, with mainly phosphate or silicate together with a mix of copper metal, copper(II) oxide and copper(I) chloride. The residues from leaching with ammonium nitrate showed that the copper speciation was similar in both residues, containing a mix of mainly phosphate or silicate together with a mix of copper(II) oxide and copper(I) chloride. The results showed that the chemical speciation may be an important factor affecting the release of copper. This work also included the collection of XAS-data for a large number of copper compounds that could possibly be present in ashes. This collection of XAS-data will be useful in future work.

Keywords: MSWI ash, copper compounds, metal speciation, XANES, EXAFS, X-Ray absorption spectroscopy

List of publications

This thesis is based on the following appended papers:

I. Lassesson, H. and Steenari, B-M. *Speciation of Cu in ash from a fluidized bed boiler fired with municipal solid waste.*
Submitted to Energy & Fuels

Contribution: Main author, almost all experimental work, data treatment, evaluation and main part of writing the manuscript.

II. Lassesson, H., Karlfeldt Fedje, K., Norén, K. and Steenari, B-M. *Leaching for recovery of Cu from MSWI fly ash – influence of ash properties and metal speciation.*
In manuscript

Contribution: All work related to copper speciation through XAS, part of writing the manuscript..

Related publication (not included in this thesis):

Lassesson, H. and Steenari, B-M. *Possibilities of ash speciation with synchrotron based x-ray absorption spectroscopy (XAS).* Proceedings of 21st International Conference on Fluidized Bed Combustion, Naples (Italy) June 3-6, 2012.

Table of Contents

1 Introduction 1

1.1 Objective 3

2 Synchrotron radiation 5

2.1 XAS 5

2.2 XANES 7

2.3 EXAFS 7

3 Analytical method 13

3.1 Description of ash samples 14

3.2 High temperature reactions of some copper species 17

4 Results 19

4.1 Speciation of Cu in BFB MSWI ashes (Paper I) 19

4.1.1 Bottom ash 22

4.1.2 Filter ash 22

4.1.3 Hopper ash 23

4.1.4 Cyclone ash 24

4.2 Influence of Cu speciation on leaching yield from MSWI fly ashes (Paper II) 24

4.2.1 Ash A – BFB fly ash 26

4.2.2 Ash B – mass burn fly ash 26

4.2.3 Residual A – after NH_4NO_3 leaching 26

4.2.4 Residual B – after NH_4NO_3 leaching 26

4.2.5 Acid leaching 27

4.3 Reactivity of copper 27

4.3.1 Mixed copper chromium oxides 28

5 Discussion 29

5.1 Evaluation methods 31

6 Conclusions 33
7 Further work 35
8 Acknowledgement 37
References 39

1 Introduction

Ever since the first humans discovered fire, there has been an increasing amount of knowledge collected about how the use of combustion for heat and power production can be made effective and how it affects the environment and human health. But still, there are things to learn. In today's society the efforts to move away from fossil based heat and power production has led to an increase in combustion of bio fuels and waste derived fuels, which brings on new challenges and new discoveries.

At the same time, the global population and economy has been increasing leading to an increased outtake of finite resources for example metals. A large part of the finite resources from nature are only used for a relatively short while in society and thereafter lost through e.g. diffuse leaching, spreading of gases and particulates in the environment or landfilling of spent products. To create a sustainable society, it is necessary to change the handling of natural resources and the managing of the waste to a system that is manageable by nature for many generations to come. It is also necessary to do this in a way that is socially and economically feasible which is a serious challenge. There are several techniques that can be used to reach a more sustainable society, which all basically leads to a reduction of material flowing through society, an increased reuse and recycling of materials and, when none of the former is possible, at least a recovery of the energy from the material. A final option is to dispose of the material in a controlled way.

The materials that are incinerated will be converted to flue gases and ashes. Ashes are complex mixtures of uncombusted material, minerals, inorganic salts and metals of which some could be recycled. There are basically three parts of an ash that could be utilized; (1) the bulk material, which could be used as a filling material, replacing sand and gravel, (2) nutrients such as phosphorous, potassium and calcium, (3) valuable trace metals (e.g. Cu, Zn, Ni, Pb). Depending on the type of fuel used, the type of incinerator and how the ash is collected, the composition of the ash bulk as well as the chemical speciation of different constituents will vary. Unfortunately, there will also be a varying amount of toxic compounds present, e.g. from some of the trace metals and some organic pollutants such as dioxins.

Copper has been identified as one of the most important elements contributing to dioxin formation within the boiler. It has been observed that $CuCl_2$ is an active catalyst while $CuSO_4$ is less active. The $CuCl_2$ can act as a catalyst for the conversion of HCl and O_2 into Cl_2 and H_2O. Subsequently, the Cl_2 can chlorinate aromatic molecules. Additionally $CuCl_2$ can act as a "shuttle" by releasing one of its Cl directly to the aromatic molecule. Through re-oxidizing by O_2 and re-chlorination by HCl, the CuCl can return to $CuCl_2$. (Wikström, 1999, Stanmore, 2004)

Recycling of ashes as a filling material in road and ground construction could substitute for virgin materials such as crushed rock. Utilization of ashes from biomass combustion as a nutrient source, in e.g.

forestry, could bring back some of the nutrients contained in the harvested biomass. According to life-cycle assessments (Toller et al., 2009) both of these scenarios save natural resources and energy, but there is also a risk for leaching of copper and other trace elements.

Removal and recovery of metals from municipal solid waste incineration (MSWI) ashes is possible, which has been shown by e.g. Schlumberger and co-workers (2007) and Karlfeldt Fedje and co-workers (2010). A process for recovery of Zn from ash, by acidic leaching followed by solvent extraction was described by Schlumberger and co-workers. This process is now being implemented at combustion plants in Switzerland. Karlfeldt Fedje and co-workers has proposed two processes for recovery of Cu from MSWI fly ashes, using leaching and separation by solvent extraction (Karlsson et al., 2010, Karlfeldt Fedje et al., 2012). One of the processes included an acidic leaching of several metals from the ash. The other process included an ammonium leaching which resulted in a more selective removal of copper. The fractions of copper released in these leaching processes varied significantly between ashes. These results could not be explained by differences in combustion technique or fuel composition, without a better understanding of the chemical speciation of copper in the ashes. One of the papers included in this thesis (Paper II) presents an investigation of the speciation of copper in two ashes from the work of Karlfeldt Fedje and co-workers (2012).

With an increased knowledge of the chemistry of trace elements (e.g. Cu) in combustion and in the ashes, it might be possible to reduce the amount of dioxins formed and thereby reducing the toxicity of the ashes as well as the flue gases. It could also increase the understanding of how to choose the best management scenario of different ashes, and support the development of recycling techniques.

Unfortunately, due to the detection limits of commonly available analytical methods (e.g. XRD) combined with low concentrations of copper, the identification of copper compounds in ashes is difficult to achieve. Selective sequential extraction protocols (Tessier et al., 1979, Van Herck and Vandecasteele, 2001) have been heavily relied on so far for speciation of metals in solid samples, such as soil and ash. The sequential extraction will, however, lead to chemical and physical alterations in the major matrix compounds and thereby also chemical transformation of the trace metal compounds. The experimental results will be significantly influenced due to these processes (Fernández Alborés et al., 2000, Funatsuki et al., 2012).

Synchrotron based X-ray absorption spectroscopy (XAS), on the other hand, is an alternative method that can be applied to the solid material without the need for dissolution or heating of the sample. XAS is element specific and gives low detection limits as well as an insignificant influence from the bulk matrix.

Some results from speciation of copper in ashes by XAS can be found in literature (Hsiao et al., 2001a, 2001b, 2002, 2006, 2007, Huang et al., 2007, Tuan et al., 2010, Takaoka et al., 2005a, 2005b,

2008, Tian et al., 2009). In most of these investigations only the fly ashes were studied. The results indicate that copper(II) is the most common oxidation state in fly ashes and that oxides, hydroxides, chlorides and sulphates are the most common compounds, in varying concentrations.

1.1 Objective

The aim of this PhD project is to contribute to the understanding of the chemistry of trace metals (e.g. Cu) in an incinerator and the chemical speciation of those trace metals when they finally end up in different ash streams. The results obtained can facilitate the development of recycling methods for metals available in ashes from combustion and thus also contribute to a minimization of the toxicity of the ashes.

The work presented in this thesis focuses on copper; the interactions between some copper minerals and other minerals and the speciation of copper in a few municipal solid waste incinerator (MSWI) ashes. An additional objective was also to discuss how synchrotron based X-ray absorption spectroscopy can be used for trace metal speciation in ash.

2 Synchrotron radiation

A synchrotron is a ring like structure with high vacuum, where charged particles travel at relativistic speeds (close to the speed of light). When a charged particle is accelerated, a photon is emitted. The acceleration of charged particles within a synchrotron happens whenever they pass through a magnetic field, e.g. from the bending magnets that keep the particles within the ring. It can also happen in so called wigglers and undulators, which are sections with several magnets placed directly after each other with fluctuating polarity making the particles travel in a zigzag pattern. Every time a charged particle accelerates back and forth in this zigzag pattern, a photon is emitted. Through this process, a more intense beam is created from the wigglers and undulators than what is possible from a bending magnet. The photons emitted will have varying wavelengths, similar to white light but not only within the visible spectrum. It is in fact possible to generate photons within the entire electromagnetic spectrum.

Before the beam of photons is used for x-ray absorption spectroscopy, it is filtered to a single wavelength with the help of a monochromator. The monochromator used in these experiments consists of two parallel crystals, where the light is scattered according to Bragg's law,

$$n\lambda = 2d\sin\theta \qquad (1.)$$

The position of the crystals will define the angle of scattering, θ, since the beam passes through a narrow opening after the second crystal. After scattering in the first crystal, the light will have multiple wavelengths due to the factor n (integer) in Bragg's law. The higher harmonics, from $n > 1$, are filtered out in the second crystal through a slight offsetting of the angle of the crystal. To record an XAS spectrum, a range of wavelengths will be needed. This is achieved by turning the crystals and thereby changing the angle θ.

2.1 XAS

Synchrotron based X-ray absorption spectroscopy (XAS) is a non-destructive, element specific, measuring technique, which requires only small amounts of sample. This means that it is possible to use the same sample multiple times and for other measurements. The bulk of the sample has only minor effects on the measured absorption data of a trace element, in that it gives some background noise. The technique is further described by Penner-Hahn (1999) and Jalilehvand (2000) among others.

All elements absorb X-rays, with higher absorption for heavier elements and decreasing absorption for increasing photon energy. The absorption is generally a smoothly declining function of the X-ray energy, except at certain energy levels that gives rise to an absorption edge, where the absorption increases drastically. This absorption edge occurs at an energy level corresponding to the binding energy of an inner electron (usually K or L shell) for an element present in the sample. The threshold energy (E_0)

is the minimum energy required to excite one of these inner electrons to continuum, i.e. create a photoelectron. By varying the photon energy over the absorption edge for a specific element, it is possible to record an absorption curve similar to Figure 1. The first inflection point of the Cu metal K-edge, marked as E = 8979 eV in Figure 1, is linked to the 1s-4p electronic transition and is usually used for energy calibration since it is easy to define. The threshold energy (E_0) is located at a slightly higher energy.

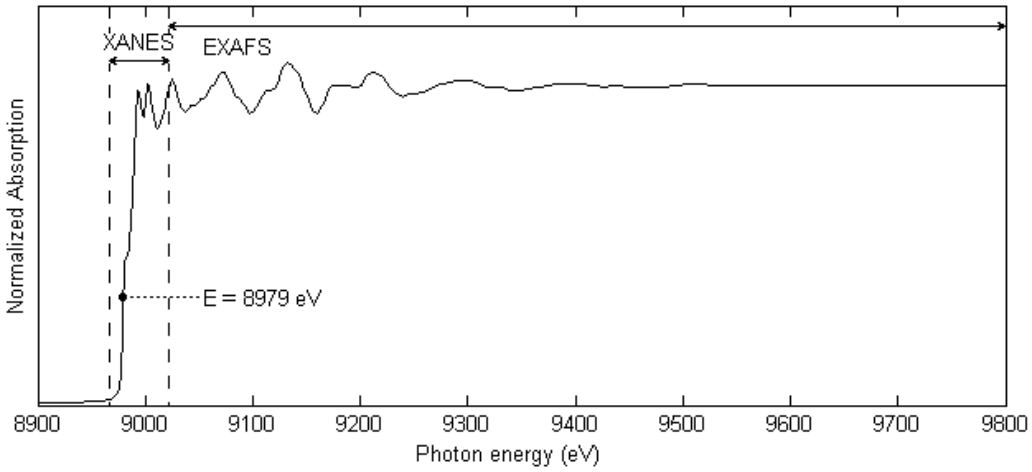

Figure 1: K-edge X-ray absorption spectrum of Cu metal, showing the XANES and EXAFS regions. Marked in the figure is the first inflection point, which is calibrated to *E*=8979 eV.

Traditionally the absorption spectrum is divided into two regions, XANES (X-ray Absorption Near Edge Structure) and EXAFS (Extended X-ray Absorption Fine Structure), marked in Figure 1. The theory describing the processes giving rise to the spectrum features is continuously being developed and it is possible to divide the spectrum in more regions. However, in the application of XAS analysis in the present work only these two regions are used.

- For $E<E_0$, the probability for x-ray absorption is low, except for electronic transitions within the atom to available energy levels, which can give rise to pre-peaks.
- For $E\approx E_0$, electronic transitions occur, with high probability, to unoccupied bound states or continuum states.
- For $E>E_0$, electronic transitions occur to continuum states and a photoelectron is ejected with kinetic energy $E_k=E-E_0$.

2.2 XANES

The edge position will be affected by oxidation state of the absorbing atom. A higher oxidation state can move the position of the edge by several electron volts towards higher energy, due to stronger interactions between the electrons and the nuclei. The pre-edge structure will be affected by coordination geometry, due to differences in energy levels in the valence shell. All of this results in a characteristic XANES region. Figure 2 illustrates how differences in energy levels can affect the XANES region. Electronic transitions are marked in the figure. In the linear two-coordinate Cu_2O, the unoccupied $4p_x$ and $4p_y$ orbitals have a lower energy than the degenerate energy level of the $4p_x$, $4p_y$ and $4p_z$ orbitals in the four-coordinate distorted tetrahedral CuCl. The Cu(II) compound has an even higher energy difference between its 1s energy level and the unoccupied 4p energy level, illustrated by $CuSO_4 \cdot 5H_2O$ in Figure 2. It has an additional unoccupied energy level at 3p, which can be seen from the 1s-3p electronic transition around 8978 eV, which is a forbidden transition according to the selection rule. Hence the low intensity of that pre-edge feature.

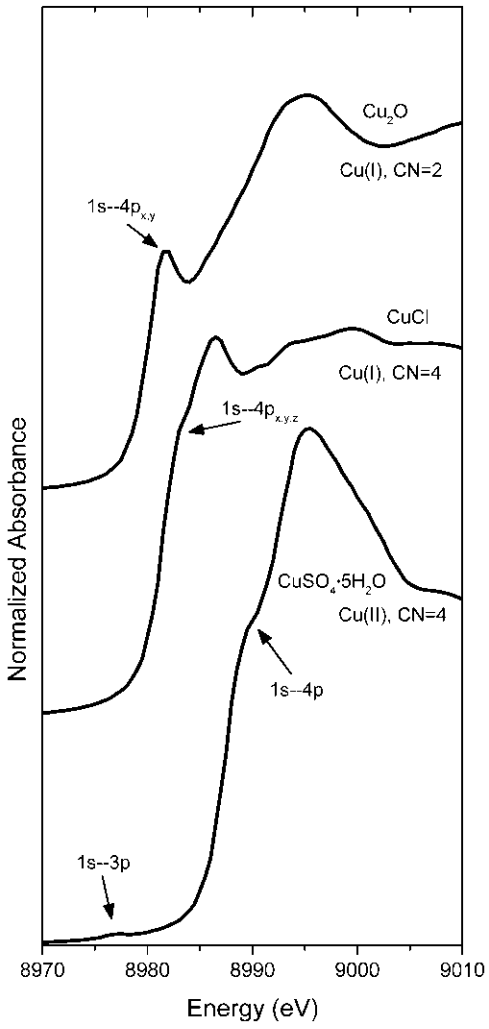

Figure 2: Pre-edge features corresponding to 1s-4p electronic transitions in Cu(I) compounds with different geometry and 1s-4p as well as 1s-3p electronic transitions in a Cu(II) compound.

2.3 EXAFS

The EXAFS region extends from about 50 eV up to more than 1000 eV above the edge. In this region photoelectrons, with kinetic energy $E_k=E-E_0$, are emitted from the absorbing atom. The photoelectrons are travelling outwards, spherically, as a wave. The de Broglie wavelength (λ_e) of the ejected photoelectron is given by the following equation:

$$\lambda_e = \frac{h}{m_e v} = \frac{h}{P} = \frac{h}{\left(2m_e E_k\right)^{1/2}} \qquad (2.)$$

where m_e is the electron mass, P is the electron momentum and h is the Planck constant. The outgoing photo electron wave can be backscattered from near-by atoms. The backscattered wave will interfere with the outgoing wave. When there is constructive interference, the electron density around the absorbing atom will increase and thereby also the photon absorption. Similarly, a destructive interference will give rise to a decrease in electron density and a decrease in photon absorption, illustrated in Figure 5. These variations in the absorption signal results in a characteristic EXAFS pattern, which is unique to the sampled specie, i.e. a "fingerprint". The EXAFS pattern contains information about distances to surrounding atoms as well as their chemical identity and abundance.

To make the EXAFS pattern more sinus shaped and easier to interpret, it is common to convert the energy scale (eV) to the photoelectron wavenumber, k (Å^{-1}), by means of the relation:

$$k = \frac{2\pi}{\lambda_e} = \sqrt{\frac{8\pi^2 m_e (E - E_0)}{h^2}} = \sqrt{0.2625 \cdot (E - E_0)} \qquad (3.)$$

It is also common to amplify the signal with a factor of k^n. Within this study k^3 was used. Figure 3 is an illustration of the EXAFS pattern of Cu metal before the conversion to k-space. Figure 4 illustrates the same pattern after the conversion to k-space.

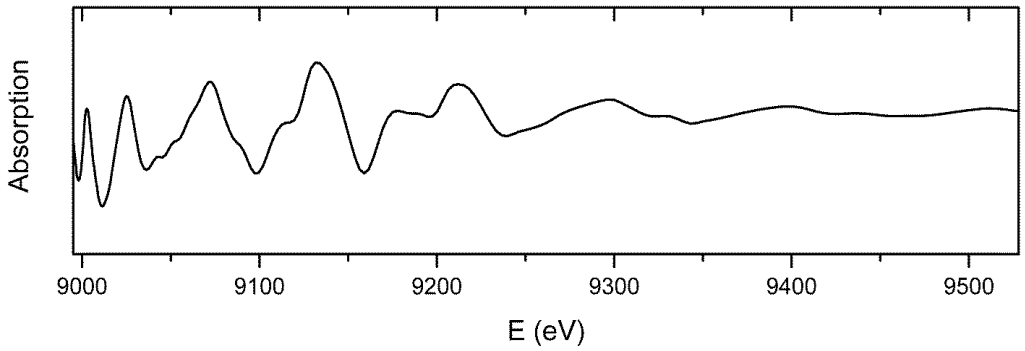

Figure 3: EXAFS pattern from Cu metal, in energy scale.

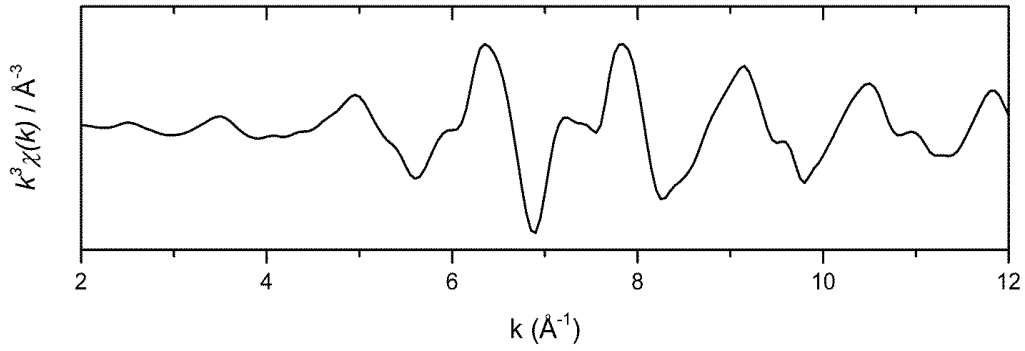

Figure 4: EXAFS pattern from Cu metal, in k-space with a k^3-amplification.

The distance (*R*) between the absorbing atom (copper) and the backscattering atom will affect the frequency of the EXAFS pattern, which is illustrated in Figure 5. For each peak in the EXAFS signal, the total number of wavelengths travelled by the photoelectron has increased by one. A small change in the kinetic energy (and thereby wavelength) of the photoelectron will have a small impact on the total number of wavelengths between the atoms when the distance is short, but a greater impact when the distance is longer. The frequency of the EXAFS pattern increases with increasing inter-atomic distance. This distance will also affect the intensity of the EXAFS pattern, which is also illustrated in Figure 5. With a larger distance, the outgoing sphere has a larger surface area and one backscattering atom covers a smaller part of that area, i.e. the probability of hitting that particular atom decreases, which in turn results in a decreased intensity of the EXAFS signal.

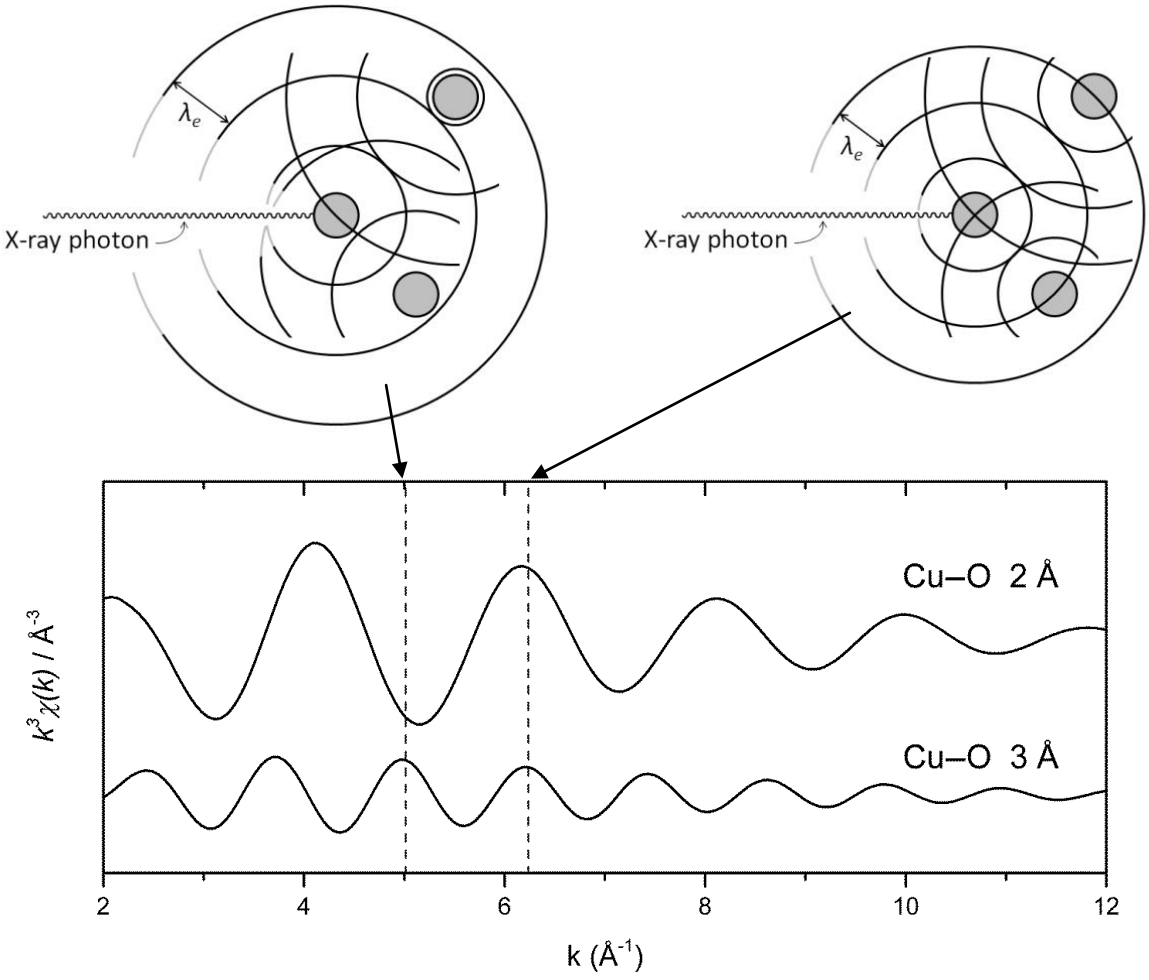

Figure 5: Schematic representation of the backscattering of Cu K-edge photoelectron waves by one oxygen atom at 2 Å and another at 3 Å (top two images) and the corresponding EXAFS pattern (bottom image). With a photoelectron wavelength λ_e = 1.25 Å there is constructive interference from the 3 Å distance, while the 2 Å results in a destructive interference (top left). With a higher photon energy, and thereby shorter photoelectron wavelength λ_e = 1.00 Å, there is constructive interference from both distances (top right).

The chemical identity (the atomic number, *Z*) of the backscattering atom can be determined from the intensity and the phase of the EXAFS signal, illustrated in Figure 6 and Figure 7. The probability for backscattering is higher for heavy elements than for light elements, which results in a higher intensity of the EXAFS signal from heavy backscattering atoms. The chemical identity will also result in a phase shift of the EXAFS oscillation (Figure 6) and in the location of the maximum intensity, also known as "the envelope" (Figure 7). The location of the maximum intensity (envelope) shifts towards higher *k*-values with increasing *Z*. It is possible to determine large differences in atomic number (e.g. Cu-Cu and Cu-O) but harder to determine when the difference in atomic number is small (e.g. Cu-O and Cu-N).

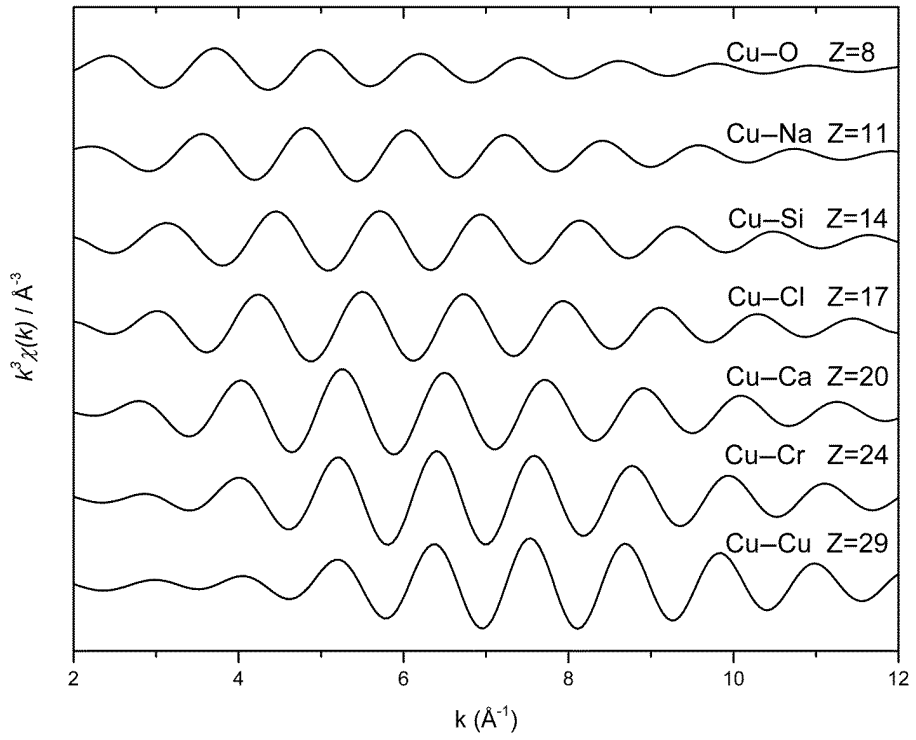

Figure 6: Theoretical $k^3\chi(k)$ functions for Cu-O, Cu-Na, Cu-Si, Cu-Cl, Cu-Ca, Cu-Cr and Cu-Cu. All signals are from one single backscattering atom at R = 3 Å, σ^2 = 0.009 Å^2. The differences in amplitude and phase make it possible to determine the chemical identity of the backscattering atom.

The abundance of neighboring atoms at a certain distance will affect the intensity, Figure 7. A higher number (*N*) of backscattering atoms will increase the probability of backscattering and consequently the amplitude will also increase with increasing *N*. The EXAFS oscillation will also be affected by the disorder among the backscattering atoms which is described by the Debye-Waller parameter (σ^2). The disorder could be due to temperature movement or configuration disorder. A higher disorder results in a larger σ^2, which in turn results in more dampening of the EXAFS oscillation,

especially at higher *k*-values, Figure 7. It is however important to remember that there is a high correlation between N and σ^2.

All of these parameters are possible to obtain from mathematical modeling based on fundamental physical properties, also known as *ab initio* modeling. The parameters obtained from the model can be compared with known crystallographic data for different compounds.

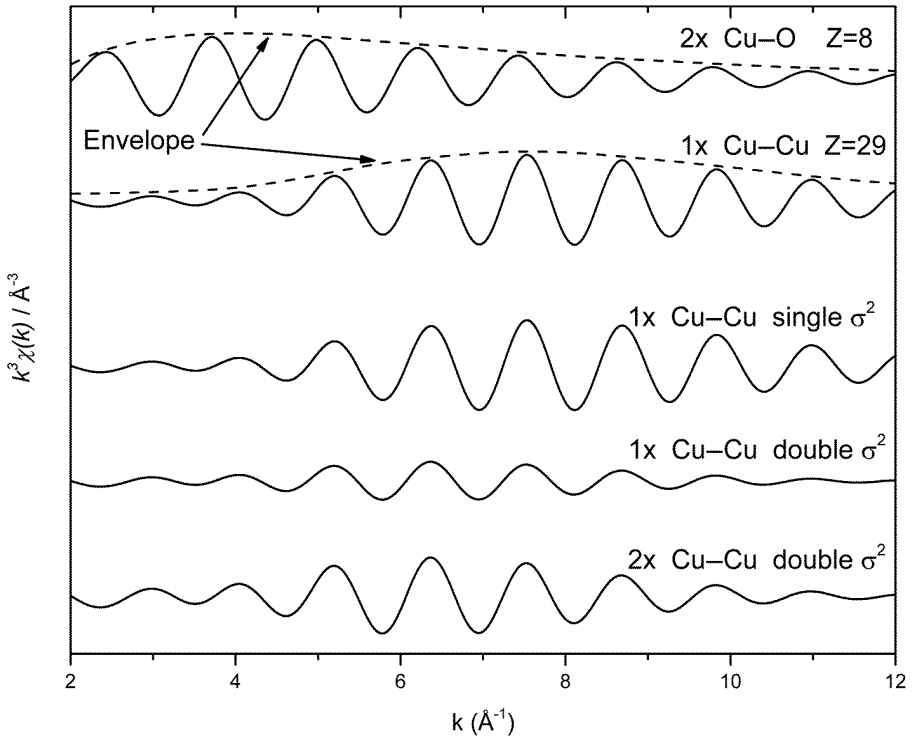

Figure 7: Theoretical $k^3\chi(k)$ functions for two Cu-O and one Cu-Cu with relating envelope at R = 3 Å, σ^2 = 0.009 Å^2, as well as one Cu-Cu with σ^2 = 0.009 Å^2, one Cu-Cu with σ^2 = 0.018 Å^2 and two Cu-Cu with σ^2 = 0.018 Å^2. All inter atomic distances are R = 3 Å.

With pure samples, containing one single compound, it is possible to determine the chemical coordination and crystal structure of that particular compound. Since ashes usually contain a mixture of several compounds of each trace metal, the information obtained will be an average of the absorption and backscattering effects of all compounds (containing the specific element) within the sample. It is usually not possible to show the exact structure of each compound within an ash sample, but it is possible to compare the sample data with crystallographic data from known compounds. There is a possibility to make approximate quantifications through *ab initio* modeling, since the coordination number, *N*, (as well as all other parameters) will be an average of all Cu atoms hit by the X-ray. It should however be remembered that the accuracy of *N* is sometimes given as low as ±25 %, but could be higher if the

conditions are right (Jalilehvand, 2000). Mixed samples, e.g. ashes, will less likely result in optimum conditions. An accuracy of N at ±25 % is probably a good estimate.

In order to improve the accuracy of the analysis in this study, the XAS data for the ash samples have been evaluated with three different techniques; comparison of the XANES region as well as the EXAFS region with data from known compounds by using linear combination fitting (LCF) and by *ab initio* modeling of the EXAFS region to achieve structural information. The methods used are described in more detail in the following section.

3 Analytical method

The element concentrations in the ash samples were determined using ICP-AES for main elements and ICP-MS for minor and trace elements after total dissolution of the ash. The main crystalline compounds in the ashes were identified by qualitative X-ray powder diffractometry (XRD) using a Siemens D5000 X-ray powder diffractometer with the characteristic Cu radiation and a scintillation detector. The identification of compounds was performed through comparison with standards in the Joint Committee of Powder Diffraction Standards.

Speciation of Cu in ash samples was investigated using X-ray absorption spectroscopy (XAS) measurements at the MAX-lab synchrotron, managed by Lund University, Sweden. In addition to data for the ash samples, XAS data were also collected for a number of model compounds that were considered possible to find in ashes. The following 18 standard compounds were used: Cu, brass, Cu_2O, CuO, $CuCrO_2$, $CuCr_2O_4$, $CuFe_2O_4$, $Cu_3(PO_4)_2$, CuCl, $CuCl_2{\cdot}2H_2O$, CuClOH/CuCl, $Cu_2Cl(OH)_3$, $Cu(OH)_2CuCO_3/CuCO_3$, $Cu(OH)_2$, $CuSO_4{\cdot}5H_2O$, $CuSiO_3{\cdot}H_2O$, $CuBr_2$ and CuS. All standard compounds were analyzed with XRD and identified as pure, i.e. < 2 % impurities, except the CuClOH/CuCl and $Cu(OH)_2CuCO_3/CuCO_3$. The CuClOH/CuCl was identified as CuClOH with a small part (≤ 7 %) CuCl. The $Cu(OH)_2CuCO_3/CuCO_3$ was identified by XRD and TGA as $Cu(OH)_2CuCO_3$ with a small part (~12 %) $CuCO_3$.

Additionally, the following compounds were used for comparison but not for identification, due to uncertainties in composition: A mixed copper calcium oxide, "CuCaOxide", and a mixed copper calcium phosphate, "CuCaPhosphate". The CuCaOxide was shown to contain several mixed oxides of copper and calcium, one example being Cu_2CaO_3. The CuCaPhosphate was identified as mostly $Ca_{21-x}Cu_x(PO_4)_{14}$, with x=1,2 or 3. Both compounds did most likely contain some impurities as well, but they were not identifiable with XRD.

Copper K-edges spectra were collected at room temperature and at ambient atmospheric pressure at beamline I811 using a Si(111) double crystal monochromator. The monochromator was detuned to 30 % below maximum intensity to remove higher order harmonics. All spectra were calibrated by assigning the first inflection point of the Cu metal K-edge to 8.979 keV. The sample spectra were collected in fluorescence mode by either a Lytle detector (ionization chamber) or a solid state (PIPS) detector and the metal foil data for energy calibration were simultaneously collected in transmission mode by ionization chambers. The intensity of the primary beam, I_0, was measured with an ionization chamber filled with N_2 to 1.1 bar. The intensity of the beam after passing the sample (I_1) and after passing the Cu metal foil (I_2) were measured with ion chambers filled with Ar to 0.1 bar and 2 bar respectively. Each XAS spectrum represents the average of two or more scans. Data processing and evaluation was carried

out using the EXAFSPAK software package (George and Pickering, 2000), as well as the Athena software (Ravel and Newville, 2005). The *ab initio* modeling of the metal species responsible for the recorded EXAFS features was done using the FEFF7 software (Zabinsky et al., 1995) and crystallographic data from the FIZ/NIST Inorganic Crystal Structure Database (ICSD, 2012).

3.1 Description of ash samples

The ash samples (bottom bed ash, ash from the bed material hopper, cyclone ash and filter ash) described in Paper I originate from combustion of MSW in a bubbling fluidized bed boiler (BFB) with a combustion temperature between 780 and 850°C. Household waste was the main fuel with minor additions of waste, e.g. plastics, wood and paper, from local enterprises. Approximately 85 % of the ferrous metal was removed from the fuel before combustion. The boiler has a lime ($Ca(OH)_2$) injection system placed before the textile filter. The boiler has been described further in (Abbas et al., 2001, 2003). The ash collection points are illustrated in Figure 8.

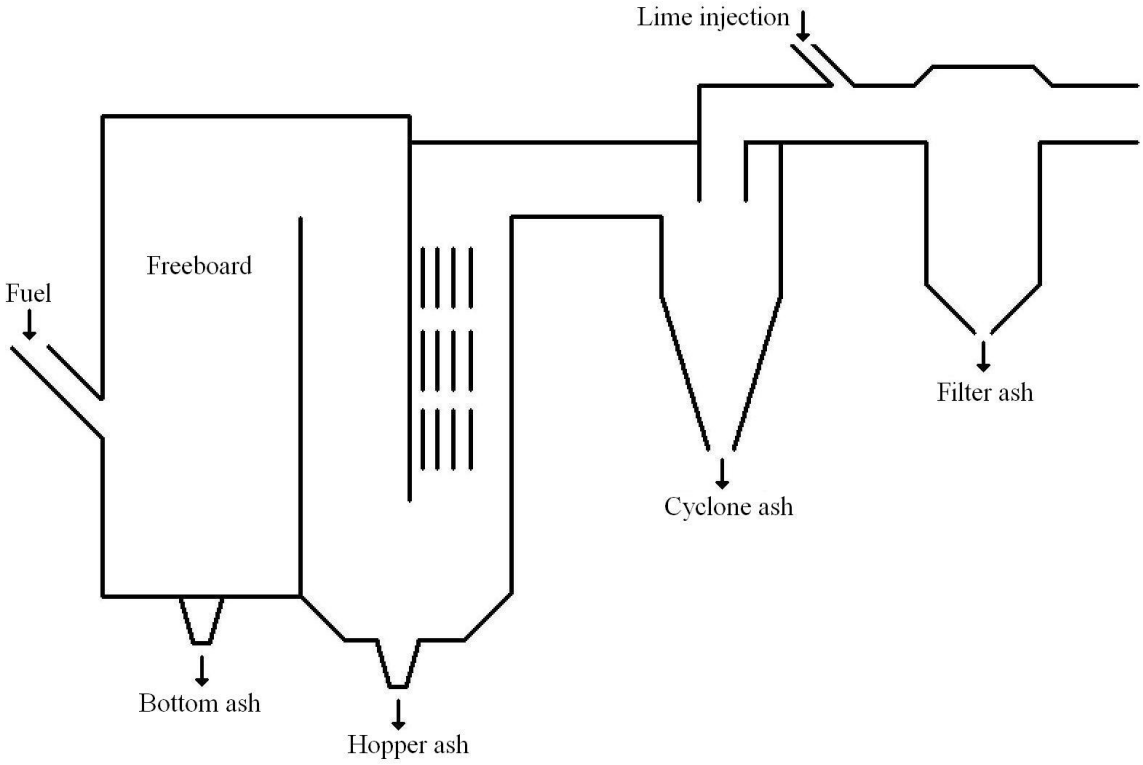

Figure 8: A schematic representation of the BFB boiler and the four ash flows.

A fly ash from the electric precipitator at a grate fired (mass burn – MB) MSWI boiler was included together with the filter ash described above in the investigation about the effect of chemical speciation on the leachability of copper in recovery processes (Paper II). The work on recovery of Cu

from these ashes was performed by Karlfeldt Fedje and co-workers (Karlfeldt Fedje et al., 2012) who investigated two processes consisting of a leaching followed by separation of copper by solvent extraction. The two procedures included leaching with either NH_4NO_3 at pH 9 or HNO_3 at pH 2.

The concentrations of elements in the ash samples studied in this work are shown in Table 1 and the main crystalline compounds present are shown in Table 2. Table 3 shows the main crystalline compounds present in the two untreated ashes as well as leaching residues discussed in Paper II. The data in Tables 1-3 has been compiled from the work of Abbas and co-workers (2001) and Karlfeldt Fedje and co-workers (2012), with a decreased number of significant digits to compensate for possible uncertainties. The XRD results are included here to give an overview of the matrix composition of the ash samples.

Table 1: Chemical composition of ash samples from the waste fired combustors. (Abbas et al., 2001, Karlfeldt Fedje et al., 2012)

Element (mg/kg dry ash)	**Bubbling fluidised bed combustor**				**Mass burn combustor**
	Bottom	**Hopper**	**Cyclone**	**Filter**	**Fly ash**
Si	330000	300000	20000	30000	70000
Al	50000	70000	120000	20000	30000
Ca	40000	50000	120000	360000	120000
Fe	21000	34000	34000	6000	24000
K	25000	20000	17000	23000	70000
Mg	6000	8000	16000	10000	12000
Mn	500	1000	2200	600	800
Na	40000	30000	30000	30000	80000
P	2000	5000	7000	4000	6000
Ti	3000	6000	7000	2000	10000
Cl	300	1500	22000	190000	110000
S	700	2000	6000	17000	75000
Cr	400	300	400	200	900
Cu	1800	3200	3200	5400	2500

Table 2: XRD results for the untreated ash samples. (Abbas et al., 2001, Karlfeldt Fedje et al., 2012)

Bubbling fluidized bed combustor ashes								**Mass burn combustor**	
Bottom		**Hopper**		**Cyclone**		**Filter**		**Filter ash**	
SiO_2	Major	SiO_2	Major	SiO_2	Major	SiO_2	Trace	SiO_2	Trace
$KAlSi_3O_8$	Major	$KAlSi_3O_8$	Major	$KAlSi_3O_8$	Major				
$(Ca,Na)AlSi_3O_8$	Major	$(Ca,Na)AlSi_3O_8$	Major	$(Ca,Na)AlSi_3O_8$	Major				
				CaO	Minor	$Ca(OH)_2$	Major	$Ca(OH)_2$	Trace
$CaSiO_3$	Minor	$CaCO_3$	Minor	$CaCO_3$	Major	$CaCO_3$	Major	$CaCO_3$	Minor
				$CaSO_4$	Minor	$CaSO_4$	Trace	$CaSO_4$	Minor
		$Ca_3Al_2O_6$	Trace	$Ca_3Al_2O_6$	Trace	$Ca_3Al_2O_6$	Trace	$Ca_3Al_2O_6$	Trace
		$Ca_2Al_2SiO_7$	Major	$Ca_2Al_2SiO_7$	Major				
		Al metal	Trace	Al metal	Major				
						CaClOH	Major		
						$KCaCl_3$	Trace		
						NaCl	Major	NaCl	Major
						KCl	Major	KCl	Minor
Fe_2O_3	Minor	Fe_2O_3	Major	Fe_2O_3	Minor				
Fe_3O_4	Minor	Fe_3O_4	Major	Fe_3O_4	Minor				

Table 3: XRD results for the untreated and leached fly ash samples. (Karlfeldt Fedje et al., 2012)

Compound	**Ash A (BFB filter ash)**			**Ash B (MB fly ash)**		
	Untreated	After NH_4NO_3 leaching (pH 9)	After HNO_3 leaching (pH 2)	Untreated	After NH_4NO_3 leaching (pH 9)	After HNO_3 leaching (pH 2)
NaCl	Major			Major		
KCl	Major			Minor		
$KCaCl_3$	Trace					
$Ca(OH)_2$	Major			Trace		
CaClOH	Major					
$CaCO_3$	Major	Major	Minor	Minor	Minor	Minor
$CaSO_4$	Trace			Minor	Minor	
$CaSO_4 \cdot 2H_2O$		Minor	Major			Major
$Ca_3Al_2O_6$	Trace	Minor	Minor	Trace	Trace	Minor
SiO_2	Trace	Trace	Trace	Trace	Trace	Minor

3.2 High temperature reactions of some copper species

As an investigation of what types of copper compounds could be expected from incineration, a thermal experiment was set up. The experiment was conducted in collaboration with and is described in more detail by (Corcoran et al., 2011). Five different copper compounds (CuCl, $CuCl_2$, $CuSO_4$, Cu_2O and CuO) where reacted individually with seven other compounds (CaO, $CaSO_4$, $Ca_3(PO_4)_2$, SiO_2, Al_2O_3, Fe_2O_3 and kaolin) in air, for 24 h, at 700 °C as well as 1050 °C. The non-copper compounds were chosen as being typical examples of ash matrix components (cf. Table 2). The samples were prepared by grinding the two powders together into a homogenous mixture. They were then allowed to react in a box-oven that held a constant temperature in air for 24 hours. The samples were analyzed by X-ray diffraction. Additionally, Cu_2O was allowed to react with Cr_2O_3 in the same way (in a tube oven).

4 Results

4.1 Speciation of Cu in BFB MSWI ashes (Paper I)

A summary of the evaluation of the XAS data of the four ash types – bottom ash, hopper ash (which is the finer particle fraction of the bed ash), cyclone ash and filter ash – are presented below. The results presented here are described in more detail in Paper I.

The suggested linear combination fitting (LCF) along with the standards suggested in the LCF, are illustrated in Figure 9 for XANES and k^3-weighted EXAFS. Results from the *ab initio* FEFF modeling of the EXAFS spectra from the ashes is gathered in Table 4, along with crystallographic data of the reference compounds in Table 5. Illustrations of the *ab initio* FEFF modeling are available in Figure 10. All percentages given within these results are atomic-percent, i.e. the number of copper atoms in a specific Cu-compound compared to the total number of copper atoms. All quantifications should be regarded as more of an approximation than an exact amount.

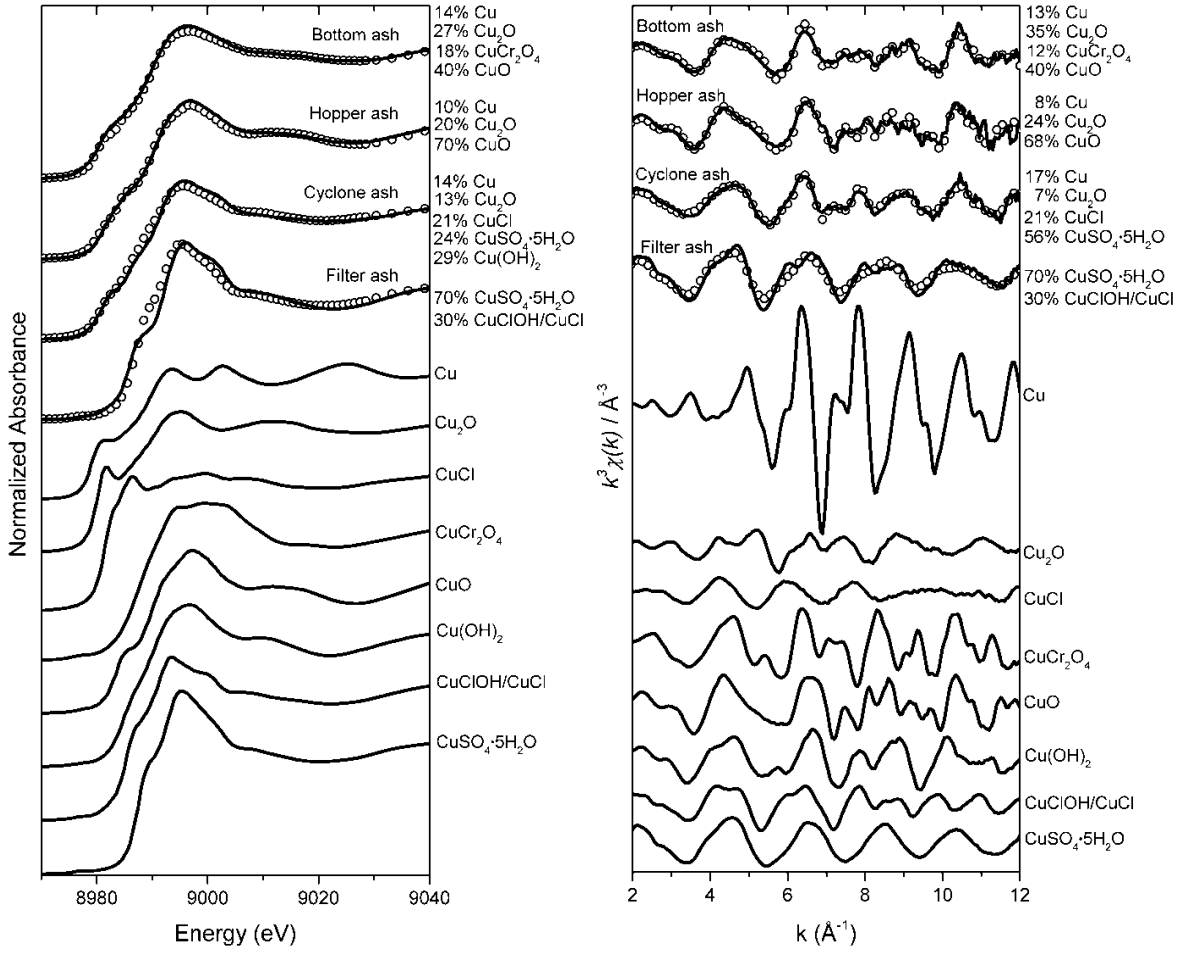

Figure 9: Cu K-edge XANES region (left) and k^3-weighted EXAFS region (right) for standards and ash samples (solid lines) with results from linear combination fitting (LCF) (rings).

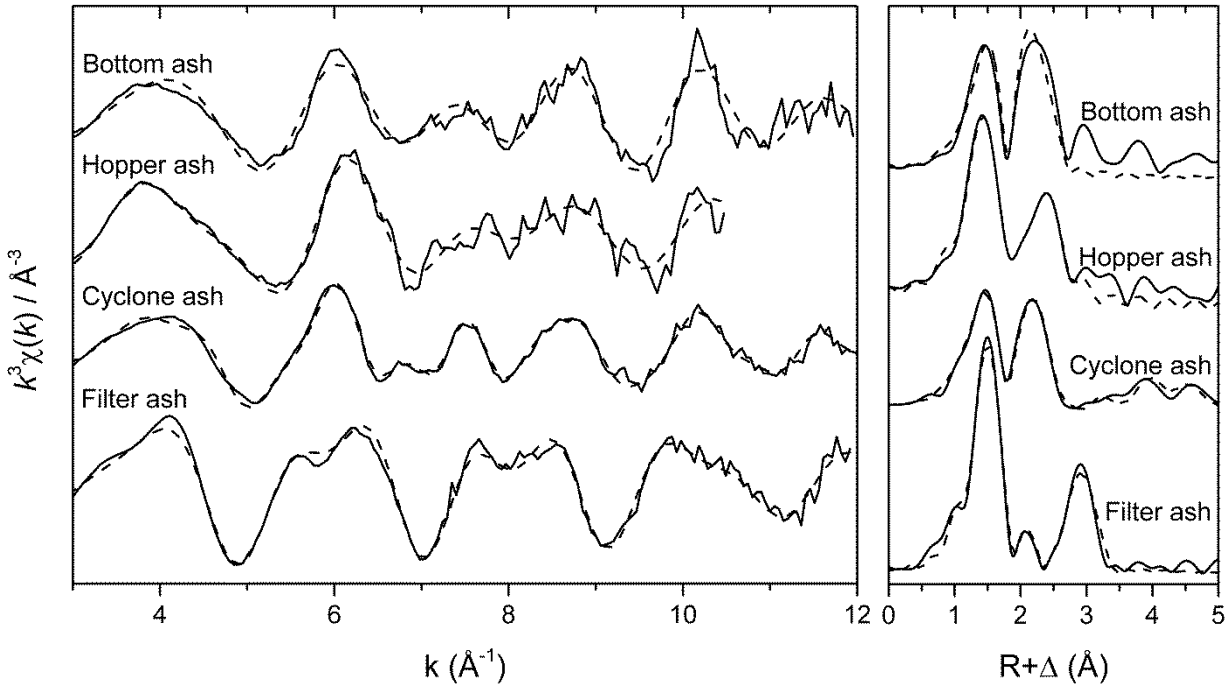

Figure 10: ***Ab initio*** **models (EXAFSPAK and FEFF7 softwares) of bottom ash, hopper ash, cyclone ash and filter ash. EXAFS signal to the left and Fourier transform of the EXAFS signal to the right (no phase shift). Solid lines are the original data and dashed lines are the model.**

Table 4: Inter-atomic distances obtained from ***ab initio*** **modeling of the sample data, with the software EXAFSPAK and FEFF7.**

Sample	**Atoms**	***R*** **(Å)**	***N***	σ^2 **(Å^2)**
Bottom ash	Cu-O	1.91	2.5	0.006
	Cu-Cu	2.56	1.3	0.005
Hopper ash	Cu-O	1.92	3.7	0.008
	Cu-Cu	2.52	0.7	0.005
	Cu-Cu	2.95	8.9	0.031
Cyclone ash	Cu-O	1.93	2.7	0.008
	Cu-Cu	2.55	1.7	0.008
	Cu-Cu	3.67	0.8	0.014
	Cu-Cu	4.47	3.3	0.014
	Cu-Cu	4.97	1.7	0.007
Filter ash	Cu-O	1.96	3.5	0.004
	Cu-Cl	2.76	1.8	0.017
	Cu-Cu	3.31	5.0	0.013

Table 5: Inter-atomic distances and coordination numbers for pure compounds suggested in the evaluation of EXAFS data. The crystallographic data was obtained from the NIST/FIZ Inorganic Crystal Structure Database.

Compound	**Atoms**	***R* (Å)**	***N***
Cu metal	Cu-Cu	2.56	12
	Cu-Cu	3.61	6
	Cu-Cu	4.43	24
	Cu-Cu	5.11	12
Cu_2O	Cu-O	1.84	2
	Cu-Cu	3.01	12
CuO	Cu-O	1.95-1.96	4
	Cu-O	2.78	2
	Cu-Cu	2.90	4
	Cu-Cu	3.08	4
	Cu-Cu	3.17	2
	Cu-Cu	3.42	2
$Cu(OH)_2$	Cu-O	1.95-1.97	4
	Cu-O	2.36	1
	Cu-O	2.92	1
	Cu-Cu	2.95	2
	Cu-Cu	3.34	4
$CuSO_4 \cdot 5H_2O$	Cu-O	1.93-1.97	4
	Cu-O	2.38-2.43	2
	Cu-S	3.55-3.68	2
CuCl	Cu-Cl	2.35	4
	Cu-Cu	3.83	12
CuClOH	Cu-O	1.98-2.02	3
	Cu-Cl	2.29	1
	Cu-Cl	2.70-2.72	2
	Cu-Cu	3.04	1
	Cu-Cu	3.29-3.39	5
$CuCr_2O_4$	Cu-O	1.99	4
	Cu-O	3.50	12
	Cu-Cr	3.46	12
	Cu-Cu	3.62	4

4.1.1 Bottom ash

The main characteristics of the XANES region of the bottom ash resembles that of a Cu(II) compound, which indicates a majority of Cu(II). There is however also an early edge region, indicating some part Cu(I) and/or Cu(0). With the help of *ab initio* modeling of the EXAFS data it was possible to identify a Cu-Cu distance of 2.56 Å, which fits perfectly with copper metal (cf. Table 5). The model suggests a coordination number N=1.3. The ash contains a mix of several copper compounds and the data from the *ab initio* model should be an average of all copper atoms present in the sample. The coordination number N=1.3 indicates that approximately 11 % of the copper atoms within the sample are part of copper metal, since a pure sample of copper metal should have N=12. The model also suggests an inner Cu-O distance of 1.91 Å, which indicates a mix of Cu(I) compounds with a typical Cu-O distance around 1.84 Å and Cu(II) compounds with a typical Cu-O distance around 1.95 Å (cf. Table 5). The best explanation to the form of the early edge in the XANES region is a mix of Cu(0) and Cu(I) with oxygen as the closest neighboring atom.

From the LCF of the EXAFS region it was also possible to distinguish a clear signal from copper metal. As can be seen from Figure 9, copper metal has a rather distinct signal and it is sufficient with a low amount of copper metal present to make it possible to see that signal. The best LCF results, which fitted rather well in both the XANES and the EXAFS regions, are illustrated in Figure 9. The LCF model of the XANES data returned 14 % Cu, 27 % Cu_2O, 18 % $CuCr_2O_4$ and 40 % CuO. The LCF of the EXAFS data returned 13 % Cu, 35 % Cu_2O, 12 % $CuCr_2O_4$ and 40 % CuO. These combinations do not fully agree with each other and the fittings do also not perfectly match the measured data, but they can be regarded as approximations or a best estimate so far. The concentrations of $CuCr_2O_4$ should most likely be lower than indicated by the LCF, since the chemical composition of the bottom ash (Table 1) shows a Cr/Cu atomic ratio of 0.16, which in turn means that the amount of $CuCr_2O_4$ could not be more than 8 % of the total amount of copper.

4.1.2 Filter ash

The XANES region of the filter ash data showed a much smaller visible early edge feature, indicating a total concentration of Cu(0) and Cu(I) lower than 5 % of the total copper content. The *ab initio* model supports this result, since it did not return any Cu-Cu distance close to 2.56 Å (i.e. copper metal) and the innermost Cu-O distance was suggested to be 1.96 Å, which is typical for many Cu(II) compounds and too large for most Cu(I) compounds (cf. Table 5). The model did also return a Cu-Cu distance of 3.31 Å, which along with the innermost Cu-O distance is found in several hydroxides, e.g. $Cu(OH)_2$ and CuClOH in Table 5. There was also a weaker signal observed at a distance between the two aforementioned. The origin of this third signal was somewhat difficult to determine but a Cu-Cl distance

at 2.76 Å was indicated as the best fit. It is quite possible that this XAS signal is actually more than one signal that could not be resolved in the data reduction.

It was hard to determine a best result from the LCF, since none of the combinations of standard spectra seemed to fit perfectly. The best fits returned combinations including $CuSO_4 \cdot 5H_2O$ in combination with hydroxides and/or chlorides. The combination of 70 % $CuSO_4 \cdot 5H_2O$ and 30 % CuClOH/CuCl gave a rather good fit in both the XANES and the EXAFS regions. It is however visually noticeable from the EXAFS region that the $CuSO_4 \cdot 5H_2O$, which is dominated by one single signal from Cu-O close to 1.95 Å, is playing a too large role in this combination. The same conclusion can be drawn from the approximate concentrations (coordination numbers) from the *ab initio* modeling. Substituting a part, or all, of the $CuSO_4 \cdot 5H_2O$ with any of the other standard compounds did however not result in a significantly better combination. The best approximation so far is that the copper compounds in the filter ash are a combination of sulfate, hydroxides and chlorides.

4.1.3 Hopper ash

There are large similarities between the XAS spectrum of the hopper ash and that of the bottom ash, which is logical since the ash collected in the hopper consists of a finer particle fraction of the bed ash. The hopper ash has less of an early edge in its XANES spectrum, compared to the bottom ash. This indicates higher concentrations of Cu(II) and less concentrations of Cu(I) and Cu(0), compared to what was found in the bottom ash. To test this theory, the bottom ash was used as one of the reference compounds for the LCF, which gave very good fits. In the LCF of the XANES region, the suggested combination was a large part bottom ash with a decrease in copper metal and an increase in CuO. In the LCF of the EXAFS region, the suggested combination was a large part bottom ash with some extra CuO. Both of these combinations give a rather good indication of what might differ between the two ashes.

A visual comparison of the EXAFS data of the hopper ash shows a great resemblance with that of CuO, for example the peaks looking like five "fingers" located at k=7-10 $Å^{-1}$. With the help of *ab initio* modeling, it was possible to find that the most prominent signal was most likely caused by a Cu-O distance at 1.92 Å. Just like for the bottom ash, this indicates a mix between Cu(II) and Cu(I) with oxygen as the closest neighboring atom (cf. Table 5). The model also showed a long Cu-Cu distance at 2.95 Å, which fits well with e.g. CuO and Cu_2O. The large σ^2 value for this signal is expected if there is a mix containing CuO and Cu_2O, since there is a large variety of distances close to 2.95 Å in a mix of these compounds. In between the two mentioned signals there was a third weaker signal which was modeled as a Cu-Cu distance of 2.52 Å, which is much too short to be anything but metallic copper.

The best linear combination fittings returned combinations of 10 % Cu, 20 % Cu_2O and 70 % CuO for the XANES and 8 % Cu, 24 % Cu_2O and 68 % CuO. Both of these combinations fit well with

each other and the information given above. The models that included the bottom ash as a reference compound did give even better results, which might indicate that some part of the copper within the two ashes is a still unknown compound. The results do however give a good approximation of the copper composition as well as the difference between the bottom ash and hopper ash.

4.1.4 Cyclone ash

The XAS spectrum of cyclone ash shares similarities with both the hopper ash and the filter ash, which is not surprising since the cyclone is located after the hopper but before the filter in the flue gas stream. The Cu K-edge shows large similarities with those of the common Cu(II) compounds, but has also got an early edge just like the bottom and hopper ashes have. The *ab initio* modeling showed a Cu-O distance at 1.93 Å, which is slightly shorter than those of most Cu(II) compounds, but still not a strong evidence for the presence of Cu(I). If there is any Cu(I) present, it is most likely just a small amount with oxygen as a nearest neighbor. The Cu-O distance at 1.93 Å does however not say anything about Cu(I) with other types of nearest neighboring atoms, e.g. CuCl or CuS. The *ab initio* model did also return a short Cu-Cu distance at 2.55 Å, which is a strong indication of metallic copper. The coordination number N=1.7 indicates an approximate concentration of 14 % metallic copper. In the spectrum part showing even larger distances there were three signals from Cu-Cu distances at 3.67, 4.47 and 4.97 Å, which all fit rather well with the distances in metallic copper (cf. Table 5). Since most other signals are hidden among the stronger signals from copper metal, it is hard to draw more conclusions from the *ab initio* modeling. With the help of LCF, with the hopper ash and filter ash as two of the reference compounds, it was possible to see some differences between the ashes. One good combination is filter ash with additional Cu metal, CuCl, Cu_2O and CuO. Another good combination is hopper ash with a decrease in CuO and increase in $CuSO_4{\cdot}5H_2O$. These results give an indication of what might be present in the cyclone ash and it gives a good indication of how the copper species changes between the ashes. Linear combination fitting, without other ashes as reference compounds, returned combinations of 14 % Cu, 13 % Cu_2O, 21 % CuCl, 24 % $CuSO_4{\cdot}5H_2O$ and 29 % $Cu(OH)_2$ for the XANES region and 17 % Cu, 7 % Cu_2O, 21 % CuCl and 56 % $CuSO_4{\cdot}5H_2O$ for the EXAFS region. As previously mentioned, these quantifications should be regarded as more of an approximation than an exact amount.

4.2 Influence of Cu speciation on leaching yield from MSWI fly ashes (Paper II)

An initial study of recovery of Cu from MSWI fly ashes, performed by Karlfeldt Fedje and co-workers (2012), investigated two processes consisting of a leaching followed by separation of copper by solvent extraction. The two procedures were tested on five different ash samples and included leaching with either NH_4NO_3 at pH 9 or HNO_3 at pH 2. The results showed that the initial dissolution and leaching is a limiting step in such a process. The leached fractions of the Cu contents ranged from 40 to 100 % of the

total content in the ashes. Detailed information about the leaching experiments and the subsequent copper separation can be found in (Karlfeldt Fedje et al., 2012). In the present work two of the ash samples and their respective leaching residues were used to investigate if the copper speciation could explain some of the differences in leaching behavior. Ash A (named "Ash 3" in Karlfeldt Fedje, 2012) released approximately 100 % of its copper in both leaching liquids, whereas Ash B (named "Ash 5" in Karlfeldt Fedje, 2012) released 60 % of its copper in both leaching liquids. Further details about chemical and physical differences of the two ashes can be found in Paper II. A more detailed discussion of the copper speciation by XAS is given here. The suggested linear combination fitting (LCF) along with the standards suggested in the LCF, are illustrated in Figure 11 for XANES and k^3-weighted EXAFS.

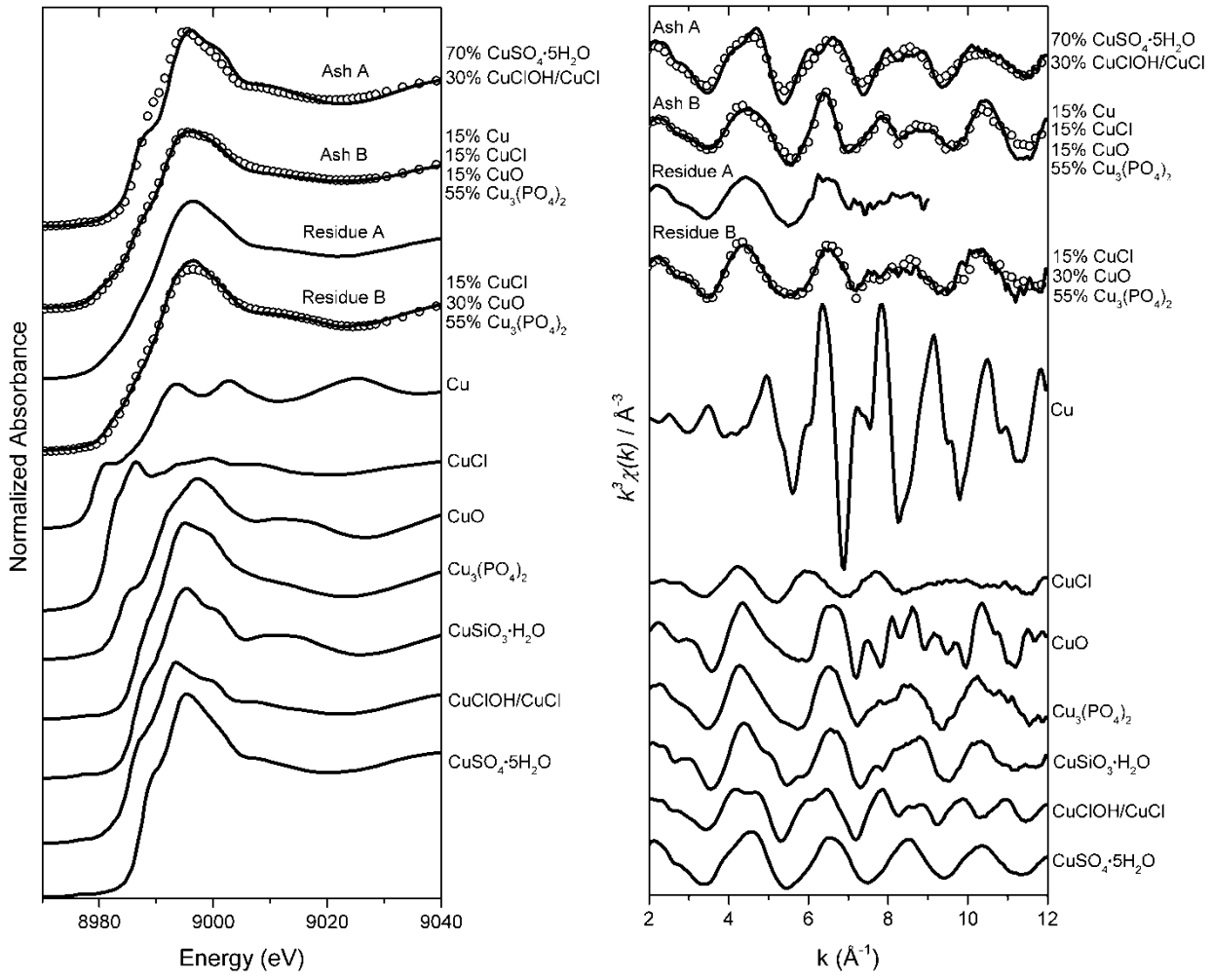

Figure 11: Cu K-edge XANES region (left) and k^3-weighted EXAFS region (right) for standards, ash samples and NH_4NO_3 leaching residues (solid lines) with results from linear combination fitting (LCF) (rings).

4.2.1 Ash A – BFB fly ash

Ash A in the work described here was taken from the same BFB boiler during the same period as the earlier four ash samples described in this thesis. Hence, the copper species are the same as in the filter ash described earlier, i.e. a mix of sulfate, hydroxides and chlorides. One linear combination fitting with 70 % $CuSO_4 \cdot 5H_2O$ and 30 % CuClOH/CuCl is illustrated in Figure 11 for the XANES and EXAFS regions.

4.2.2 Ash B – mass burn fly ash

The XAS spectra of Ash B showed similarities with Cu(II) compounds in the XANES region, with a small early edge region, indicating Cu(II) as the major part and Cu(I) and Cu(0) as smaller additions. There is a distinct pattern similar to that from metallic copper in the EXAFS region. Linear combination fitting of the EXAFS region indicates that approximately 15 % of the copper is metallic copper. Preliminary results of *ab initio* modeling suggest that the shortest backscattering distance is that of a Cu-O at 1.94 Å, which is close to a typical Cu(II)-O distance. This indicates that the concentration of Cu(I)-O from e.g. Cu_2O and $CuCrO_2$ is close to zero. Since 15 % metallic Cu is not enough to explain the early edge in the XANES region, this suggests that there might be some other Cu(I) compound, e.g. CuCl or CuS. From linear combination fitting, it was concluded that the CuCl fits better than the CuS and a model that explains both the XANES and EXAFS regions quite well includes 15 % Cu, 15 % CuCl, 15 % CuO and 55 % $Cu_3(PO_4)_2$. It was however also observed that the silicate, $CuSiO_3 \cdot H_2O$, fits almost as well as the phosphate, since their spectra are quite similar (Figure 11).

4.2.3 Residual A – after NH_4NO_3 leaching

Approximately 100 % of the copper in Ash A was released during leaching with ammonium nitrate. There was just enough left to generate a weak XAS spectrum. The spectrum is too weak and noisy for a good estimate of the copper compounds present. It does however show clear similarities with the residual from Ash B after the same leaching procedure (Figure 11). It can be concluded that they have similar copper compositions.

4.2.4 Residual B – after NH_4NO_3 leaching

The XAS spectrum of residual B, after leaching with ammonium nitrate, shows similarities with the spectra of Cu(II) compounds in the XANES region, with a small early edge indicating lower oxidation numbers as well. This small early edge does however start at a slightly higher energy than what was observed for the XAS spectrum of Ash A, more similar to what is expected of e.g. CuCl (cf. Figure 2). This observation was supported by the LCF as well as *ab initio* modeling of the EXAFS region, in which it was not possible to find any indications of metallic copper. The *ab initio* modeling did also indicate that

the shortest backscattering distance was a Cu-O distance of 1.97 Å, which suggests that there is no Cu(I) compound with oxygen as a nearest neighboring atom. From the LCF it is concluded that the phosphate fits better than the silicate, but they are still too similar to determine which one is present or not. One combination that fits quite well in both XANES and EXAFS is 15 % CuCl, 30 % CuO and 55 % $Cu_3(PO_4)_2$, illustrated in Figure 11.

4.2.5 Acid leaching

The XAS spectra of residues from the ashes leached with acid were too weak or too noisy to allow for any conclusive results.

4.3 Reactivity of copper

As described in the section 3.2 and in (Corcoran et al., 2011), five copper compounds (CuCl, $CuCl_2$, $CuSO_4$, Cu_2O and CuO) where reacted individually with seven other compounds (CaO, $CaSO_4$, $Ca_3(PO_4)_2$, SiO_2, Al_2O_3, Fe_2O_3 and kaolin) in air, for 24 h, at 700 °C as well as 1050 °C. The non-copper compounds were chosen as being typical examples of ash matrix components.

From these experiments it was observed that:

- The two chlorides evaporated at 1050 °C. At 700 °C the chlorides partly evaporated and partly transformed into CuO from reaction with oxygen in the air, corresponding with the Deacon process (Hisham and Benson, 1995).
- The $CuSO_4$ was not stable at any of the two temperatures, but decomposed to copper oxide as shown also in literature (Kolta and Askar, 1975).
- The two copper oxides are interchangeable, meaning that Cu_2O oxidizes to CuO at 700 °C in contact with air and CuO is reduced to Cu_2O with a release of oxygen at 1050 °C. The conversion of CuO to Cu_2O at 1050 °C was however not complete, indicating that the conversion might be slow at this temperature. According to Neumann and co-workers (1984) this reduction should happen just above 1030 °C in air (21 % O_2) at normal pressure.
- Mixed oxides were seen as products when copper oxides reacted with CaO at 1050 °C, with Fe_2O_3 at both temperatures and with Al_2O_3 at 1050 °C. These mixed oxides agree with previous results (Mathews et al., 1993, Jacob et al., 1977, Hu et al., 2010). The mixed oxide $CuAl_2O_4$ was also a product from reactions between copper oxides and kaolin at 1050 °C, also agreeing with Hu et al. (2010).
- Reactions with SiO_2 did sometimes result in amorphous products. It was not possible to determine, with XRD, if copper was a part of those amorphous products.

- The $CaSO_4$ was stable at both temperatures, with the exception of CuO mixed with $CaSO_4$ at 1050 °C where a small amount of mixed oxide was found. This agrees well with Ingo et al. (1998) reporting that $CaSO_4$ is stable up to about 1240 °C in a pure form, while an addition of SiO_2 and Cu_2O or CuO lowers the decomposition temperature.
- The $Ca_3(PO_4)_2$ reacted with all of the copper compounds, in fact it was the only compound that reacted with the copper chlorides at 1050 °C before the rest of the chlorides evaporated. The product was identified as $Ca_{21-X}Cu_X(PO_4)_{14}$, where x = 1,2,3. This compound has been discussed in literature earlier (Sulowska et al., 2012).

One of the mixed oxides identified in this experiment was the spinel $CuFe_2O_4$, which was later obtained as a pure compound from a reaction with CuO and Fe_2O_3 in air at 950 °C for 61 h. The XAS spectrum of this product was later used as a reference compound for linear combination fitting of XAS data. Both the copper calcium oxide and the copper calcium phosphate were also used in the XAS analysis, not for identification but for comparison. They were not used for identification due to inconclusive evidence of what they actually contained. The copper calcium oxide was identified with XRD as a mix of several copper(II) calcium oxides, but seemed to contain some Cu(I) as well according to XAS data. Impurities in the copper calcium phosphate was hard to determine exactly with XRD due to overlapping peaks, but the XAS data showed some Cu(I) as well.

4.3.1 Mixed copper chromium oxides

A similar experiment was conducted where Cu_2O was left to react with Cr_2O_3 in air, for 24 h, at 700 °C as well as 1050 °C. It was then seen that mixed oxides were the result at both temperatures, $CuCrO_2$ at 1050 °C and $CuCr_2O_4$ at 700 °C, similar to what (Stroupe, 1949) reported. The Cr/Cu ratio was unfortunately wrong at the lower temperature, so a new mix was made with correct Cr/Cu ratio which was left to react for 65 h at 700 °C, resulting in a pure $CuCr_2O_4$. The XAS spectrum of the two pure copper chromium oxides were later used as reference compounds for linear combination fitting of XAS data.

5 Discussion

The results from the BFB ashes indicate a quite low average oxidation number in the bottom ash, and an increase in oxidation state before ash is collected in the hopper. This indicates reducing conditions close to and inside the burning waste particles. The fluidizing air is just one part of the total air available for combustion. More air is introduced further up, in the freeboard, through secondary air nozzles. Larger pieces of metal will most likely have a higher tendency to remain close to the bottom of the combustion chamber, while smaller pieces are carried by the fluidizing air out of the combustion chamber into the hopper. Smaller particles have higher surface to volume ratio than the larger ones which makes reactions within them more likely to reach equilibrium within a limited time. The smaller particle size in combination with the secondary air probably explains the higher concentration of CuO in the hopper ash compared to in the bottom ash. The volatile copper chlorides were not detected in the bottom and hopper ashes, which is understandable considering the high temperatures prevalent in those parts of the boiler. The high temperatures can also explain why no copper sulfate was found in the combustor bed. Copper sulphate is not stable at temperatures above ~650 °C (Weast, 1975, Kolta and Askar, 1975).

The evaluation and modeling of the XAS data for bottom ash suggested the presence of copper chromium oxide $CuCr_2O_4$. This compound could be a result of a solid state reaction between copper oxide and chromium oxide, as was shown in the laboratory experiment where Cu_2O and Cr_2O_3 were mixed and heat treated at 700°C. This copper chromium oxide has also been identified in other ashes from combustion tests, as well as suggested as the dominating chromium compound under certain thermodynamic conditions (Lundholm et al., 2007, Lundholm et al., 2008). However, it cannot be present in higher amounts than 8 % of the total copper content of the ash due to the low Cr content in the ash. It was also observed, in the heating experiments described in this thesis, that copper can form mixed oxides with other metals, e.g. iron, calcium and aluminium, in a similar manner as for the copper chromium oxide. Those mixed oxides would give rather similar XAS spectra and could very well constitute a part of the copper mix in the bottom ash as well as in the hopper ash.

The BFB cyclone seems to be quite effective in removing the remaining pieces of metallic copper. Copper metal is found in relatively high concentrations in the cyclone ash, but none is found in the filter ash. The metallic copper found in the cyclone ash is probably not a result from reducing conditions since it has passed through the secondary air and passed by the hopper before being separated in the cyclone. The Cu(I) found in the cyclone ash could be due to surface reactions on metallic copper with oxygen or HCl. The combination of copper compounds found in the cyclone ash shows similarities with those observed for both the hopper and filter ashes, which is not surprising since the cyclone is located after the hopper and before the filter in the flue gas cleaning system.

The copper XAS data of the BFB filter ash was the most difficult to interpret with the standard compounds available. The best estimate so far is a mix of sulfate, hydroxides and chlorides. It is possible that the chlorides have travelled all the way from the furnace to the filter, initially in gaseous form and later as liquid or solid particles as the temperature decreased in the convection zone. It is also possible that chlorides were formed in the flue gas channel due to reactions between other copper compounds and HCl (Weast, 1975, Verhulst et al., 1995). The hydroxides could result from reactions with water vapor, either in the flue gas or after the ash was collected. The ash samples have been stored in air tight containers, but have been in contact with air during handling. Sulfates could have formed through reactions of e.g. copper oxide with SO_2 and O_2 in the flue gas (Gullett et al., 1992).

For the BFB cyclone ash and filter ash, the speciation efforts pointed at $CuSO_4 \cdot 5H_2O$, or a compound with a similar crystal structure. This other compound with a similar structure could be a mix of several Cu(II) compounds in which oxygen is the nearest neighboring atom to copper. Another possible explanation is the presence of defective or not fully developed crystals of one (or several) Cu(II) compound(s), or amorphous Cu(II) compounds. All of these alternatives could give rise to a similar EXAFS signal, i.e. oxygen as the nearest neighbor at a distance of ~1.95 Å and no significant FT peaks beyond that, since the second layer of atoms and beyond will in these cases not comprise distinct distances that can appear as signals in the EXAFS spectrum. In addition, hydrated compounds usually have rather large distances to the nearest heavy backscatterer (e.g. Cu) and all the lighter ones (e.g. H, O, S, Cl) will only give weak signals that are harder to detect, i.e. also similar to $CuSO_4 \cdot 5H_2O$.

The copper composition of the mass burn combustor fly ash in its untreated state was quite different from that of the BFB filter ash. The MB fly ash contained copper(II) phosphate (or silicate) combined with smaller amounts of copper(II) oxide, copper(I) chloride and copper metal, while the BFB filter ash contained a mix of copper(II) sulfate, hydroxides and chlorides. During the evaluation and modeling of the XAS data of the MB ash and the residues remaining after leaching of this ash by acid or ammonium nitrate it was noted that the speciation of copper in these samples showed clear similarities, which were not found for the BFB filter ash and it´s leaching residues. According to the speciation of the MB fly ash, approximately 100 % of the metallic copper was dissolved in the ammonium nitrate, while approximately 20 % of the CuO and 60 % of the CuCl and $Cu_3(PO_4)_2$ dissolved. The BFB filter ash contained primarily easily soluble compounds, which contributed to an almost complete removal of copper in the leaching experiments. The fact that both leaching residues of the MB fly ash showed remarkable similarities in Cu XAS data indicates that these copper compounds are sparingly soluble in both leaching liquids. It is also possible that the copper compounds remaining in the residues are physically enclosed in glassy slag particles since the temperature in the combustion zone is quite high.

The similarities between the untreated MB fly ash and the leaching residues indicate that the MB fly ash contained those compounds before treatment.

Exactly how the phosphate/silicate in the MB fly ash was formed is still not clear. Partly because it is unclear where it was formed, which could be explained by further studies of ashes from other locations in the same boiler and occasion. It is also uncertain if it is a phosphate, silicate or both. A few examples of how copper phosphates can be formed through heating of copper compounds along with other (less stable) phosphates are described by Bamberger and co-workers (1997) or as a part of a phosphate glass described by Pickup and co-workers (2006). It was also noted in the present work that heating of combinations of copper compounds and calcium phosphate resulted in a mixed phosphate, which showed less similarities with the MB fly ash than the $Cu_3(PO_4)_2$ did. It was however also concluded that the sample of mixed phosphate most likely contained impurities. One possible route to forming silicate like copper compounds is through partial melting of glass particles along with copper compounds inside the incineration chamber. Sulowska and co-workers (2012) could for example detect a crystalline $Cu_{0.69}Mg_{1.31}Si_2O_6$ formed from heating of a CuO-containing silicate-phosphate glass. Glass can occur in many forms and it is a common part of MSW and it can be found in droplet like formations in the bottom ash, indicating that melt has occurred. Dust from such glass particles could have travelled all the way to the flue gas cleaning system as the metallic copper did. If this is how a possible copper silicate was formed, then it should be possible to detect the same compound in the bottom ash as well. Other techniques, e.g. SEM-EDX, are also a possibility for determining the chemical surroundings of copper. Further studies are needed to determine the origin of the copper phosphate/silicate in the MB fly ash.

It was difficult to reach a conclusion, with high certainty, on the copper speciation for some samples. Partly, this was due to similarities between the reference compounds, e.g. phosphate and silicate. It could also be due to a lack of some reference compounds, although the database was quite extensive. There is also a possibility that some of the copper compounds in the ash samples were not well crystallized. Defective or small crystal units (crystallites) can give an XAS spectrum that differs from that of the well crystallized one. This could be a result of rapidly formed compounds. Since copper can be involved in many transformations in the combustion chamber and the flue gas system, it is probable that the ashes contain rapidly formed copper compounds and that could explain the diffuse XAS spectra observed for some samples.

5.1 Evaluation methods

An important part of this work has been to learn how to make qualified copper speciation of mixed compounds with the help of synchrotron based X-ray absorption spectroscopy. Some of the experiences, so far, are explained here.

When the XAS spectra is converted into a more sinus shaped EXAFS pattern, it involves a conversion into *k*-space ($Å^{-1}$), by means of the relation

$$k = \sqrt{0.2625 \cdot (E - E_0)} \qquad \text{(from equation 3.)}$$

where E and E_0 are expressed in eV. This means that the EXAFS pattern is dependent on the position (value) of E_0. All compounds have different E_0 values, which is often derived from the first inflection point of the XAS edge. In order to make their spectra comparable on the same *k*-scale, it is necessary to set E_0 for all standard compounds and the sample to the same value before LCF of the EXAFS pattern is conducted.

In this work it was observed that using more than one method for evaluation of metal XAS data can make it easier to reach a probable result in terms of metal speciation. The methods linear combination fitting of XANES spectra and EXAFS data separately as well as doing *ab initio* modeling of the atomic distances indicated by the EXAFS data gives complementary results. With the help of LCF of the XANES spectra, it is possible to detect differences in oxidation numbers, but it is sometimes hard to determine the exact concentrations of Cu(0) and Cu(I) if both are present since they are somewhat overlapping. There are also similarities between the spectra for some Cu(II) compounds which makes it difficult to identify them with certainty in a mix of copper compounds. Metallic copper shows a strong signal in the EXAFS region and can be approximately quantified from that. The shortest Cu-O distance given by *ab initio* modeling of EXAFS data will also give a hint about concentrations of Cu(I) and Cu(II), where a shorter distance indicates more Cu(I) and longer distance indicates more Cu(II) (cf. Table 5). It is, however, important to remember that copper compounds with any other nearest neighboring atom besides oxygen will give different results. Linear combination fitting and *ab initio* modeling of EXAFS data will most likely give similar results since they are based on the same data, i.e. one should not be seen as a confirmation of the other. While the EXAFS pattern contains information about distances to surrounding atoms as well as their chemical identity and abundance, the XANES data is based on somewhat different properties in the sample, such as electron transitions and oxidation states. If a combination fits in both the XANES and the EXAFS regions, it is more likely to be a good fit than if it only fits in one of the regions.

By using other ashes as reference compounds in the LCF, it was possible to observe and evaluate similarities between some ashes as well as differences. This could sometimes help in the identification of copper compounds. It could also help in the understanding of what reactions might have occurred in different parts of the boiler.

6 Conclusions

The speciation of copper compounds in the ash samples from the BFB boiler showed the occurrence of mainly oxides early in the process (in or close to the bed) and more of sulfate, chloride and hydroxide later in the process (in or close to the filter). These observations are consistent with the volatility of the respective copper compounds and reactions with gases. Copper metal was found in small amounts in several parts of the boilers, which is consistent with small metal pieces travelling with the flue gas flow and reacting slowly.

The results obtained in this work give a complete picture of the speciation of copper in different parts of a fluidized bed combustor. No similar investigation has been found in the literature. The present results can be used to get indications of reactions involving copper species in combustion of waste. However, the exact speciation of copper in the waste, i.e. the fuel, is still not known and therefore the starting point for the reaction mechanisms cannot be stated yet.

The copper speciation of the fly ash from the mass burn combustor showed large differences from that of the bubbling fluidized bed combustor filter ash. The observations showed that the copper speciation in the mass burn fly ash, which contained compounds with low solubility in acid and ammonium nitrate, was hindering full recovery of copper from that ash (≈60% released). The BFB filter ash copper speciation showed only compounds with high solubility which was consistent with the high copper yield from leaching (≈100%). This is an important piece of information that has not been discussed in the literature earlier. Results like these can be used to support the design of a recovery method for copper from MSWI fly ash since the efficiency of such methods is dependent on the chemical state and solubility of the copper in the ashes to be treated. Data for ash samples from more combustors will be gathered in future work in order to get reliable statistics.

Speciation based on XAS data of metal compounds in complex samples such as ashes requires access to XAS data for all pure compounds that can be present in the sample. This work included the collection of XAS-data for a large number of copper compounds that could possibly be present in ashes. The number of reference compounds used in this work is significantly larger than what has been found in other publications. Even so, it was found during the work presented in this thesis that even more copper compounds can be present. Mixed oxides and different silicates are examples of such compounds which will be investigated further in future work.

7 Further work

This work includes a limited number of ashes. However, already with this limited number of ashes it was possible to see that the copper speciation within the ashes changed with different incineration scenarios. It is however not possible to draw any conclusions about how the copper speciation will shift in yet another incineration scenario. There is a multitude of factors that could change between different incineration scenarios and within this study almost all of those factors were altered. With the help of a larger selection of ashes it might be possible to see the significance of these factors. This larger selection of ashes should include ashes from all collection points of a boiler during a given incineration scenario and they should include as many incineration scenarios as possible. Chalmers research boiler (CFB) represents a good opportunity since it is possible to change one parameter at a time, e.g. changing the fuel mix without changing the incinerator and the combustion parameter settings.

When the copper speciation of a large selection of ashes has been identified, a complete statistical analysis will be needed. This analysis should include as many parameters as possible, to detect any patterns in how the copper speciation changes with incineration scenarios. By doing so it might be possible to predict the copper speciation of a particular ash before it is created, just by knowing e.g. where and how the incineration takes place, what type of fuel is used and how the ash is collected.

Thermodynamic modeling of the incineration scenarios will also help in the understanding of what parameters that will have a large effect on metal speciation in the ashes. Thermodynamics can also explain where the critical thresholds might be of certain parameters.

Within this study a few question were raised, e.g. whether it was phosphate or silicate in the MB fly ash. This question could be answered with the help of a SEM-EDX study, where the chemical surrounding of copper containing particles is further studied. This could also explain whether the copper speciation is the limiting factor in leaching or if the copper is enclosed in some other insoluble substance.

The speciation results thus obtained will be discussed in relation to the work on development of processes for metal recovery from MSWI ash carried out at Industrial Materials Recycling Chalmers.

8 Acknowledgement

This work has been funded by Formas (The Swedish Research Council for Environment, Agricultural Sciences and Spatial Planning), Swedish Energy Agency and Chalmers Area of Advance Energy which is gratefully acknowledged. It has been carried out within the graduate school Polytechnic Waste Research in Sweden-POWRES, also funded by FORMAS.

I would like to send out a few special thanks to

- Dr. Stefan Carlson at beamline I811 and the Maxlab staff for making the XAS measurements possible.
- Dr Katarina Norén at MaxIV Laboratory, Lund and Professor Ingmar Persson, Swedish Agricultural University, Uppsala for helpful discussions around XAS.
- My examiner Christian Ekberg for interesting discussions around almost anything but XAS.
- My supervisor Britt-Marie Steenari for all her support and patience and for making me feel comfortable as a PhD student.
- Angelica Corcoran, Anna Emanuelsson, Joel Hedlund, Filip Holmberg and Markus Jansson for your contribution to the study of reactivity of copper.
- All my co-workers at Nuclear Chemistry and Industrial Materials Recycling, Chalmers, for making me feel comfortable, even though I was a physicist among chemists.
- All my co-workers at Inorganic Environmental Chemistry, Chalmers, for making me feel welcome and for letting me use some of your equipment.

Last but not least I would like to thank my wife, family and friends for all support you have given me during my studies and for bearing with me and being there for me when I needed you during this harsh period of thesis writing.

References

ABBAS, Z., MOGHADDAM, A. P. & STEENARI, B. M. (2003) Release of salts from municipal solid waste combustion residues. *Waste Management,* 23**,** 291-305.

ABBAS, Z., STEENARI, B. M. & LINDQVIST, O. (2001) A study of Cr(VI) in ashes from fluidized bed combustion of municipal solid waste: Leaching, secondary reactions and the applicability of some speciation methods. *Waste Management,* 21**,** 725-739.

BAMBERGER, C. E., SPECHT, E. D. & ANOVITZ, L. M. (1997) Crystalline copper phosphates: Synthesis and thermal stability. *Journal of the American Ceramic Society,* 80**,** 3133-3138.

CORCORAN, A., EMANUELSSON, A., HEDLUND, J., HOLMBERG, F. & JANSSON, M. (2011) Copper compounds' reactions with mineral - in air at 700 and 1050 °C (in Swedish). *Department of Chemical and Biological Engineering.* Gothenburg, Sweden, Chalmers University of Technology.

FERNÁNDEZ ALBORÉS, A., PÉREZ CID, B., FERNÁNDEZ GÓMEZ, E. & FALQUÉ LÓPEZ, E. (2000) Comparison between sequential extraction procedures and single extractions for metal partitioning in sewage sludge samples. *Analyst,* 125**,** 1353-1357.

FUNATSUKI, A., TAKAOKA, M., OSHITA, K. & TAKEDA, N. (2012) Methods of determining lead speciation in fly ash by X-ray absorption fine-structure spectroscopy and a sequential extraction procedure. *Analytical Sciences,* 28**,** 481-490.

GEORGE, G. N. & PICKERING, I. J. (2000) EXAFSPAK - A Suite of Computer Programs for Analysis of X-ray Absorption Spectra. Stanford, CA, SSRL.

GULLETT, B. K., BRUCE, K. R. & BEACH, L. O. (1992) Effect of sulfur dioxide on the formation mechanism of polychlorinated dibenzodioxin and dibenzofuran in municipal waste combustors. *Environmental Science & Technology,* 26**,** 1938-1943.

HISHAM, M. W. M. & BENSON, S. W. (1995) Thermochemistry of the Deacon Process. *The Journal of Physical Chemistry,* 99**,** 6194-6198.

HSIAO, M. C., WANG, H. P., CHANG, J. E. & PENG, C. Y. (2006) Tracking of copper species in incineration fly ashes. *Journal of Hazardous Materials,* 138**,** 539-542.

HSIAO, M. C., WANG, H. P., HUANG, Y. J. & YANG, Y. W. (2001a) EXAFS study of copper in waste incineration fly ashes. *Journal of Synchrotron Radiation,* 8**,** 931-933.

HSIAO, M. C., WANG, H. P., PENG, C. Y., HUANG, C. H. & WEI, Y. L. (2007) Chemical structure of copper in incineration dry scrubber and bag filter ashes. *AIP Conference Proceedings.*

HSIAO, M. C., WANG, H. P., WEI, Y. L., CHANG, J.-E. & JOU, C. J. (2002) Speciation of copper in the incineration fly ash of a municipal solid waste. *Journal of Hazardous Materials,* 91**,** 301-307.

HSIAO, M. C., WANG, H. P. & YANG, Y. W. (2001b) EXAFS and XANES Studies of Copper in a Solidified Fly Ash. *Environmental Science & Technology,* 35**,** 2532-2535.

HU, C.-Y., SHIH, K. & LECKIE, J. O. (2010) Formation of copper aluminate spinel and cuprous aluminate delafossite to thermally stabilize simulated copper-laden sludge. *Journal of Hazardous Materials,* 181**,** 399-404.

HUANG, Y. C., WANG, H. P., HUANG, H. L., HUANG, Y. J., CHANG, J. E. & WEI, Y. L. (2007) Speciation of copper in plasma-melted slag. *Journal of Electron Spectroscopy and Related Phenomena,* 156-158**,** 214-216.

ICSD (2012) Inorganic Crystal Structure Database 1.9.1 (release 2012-2). FIZ/NIST: Gaitensburg, MD.

INGO, G. M., CHIOZZINI, G., FACCENDA, V., BEMPORAD, E. & RICCUCCI, C. (1998) Thermal and microchemical characterisations of $CaSO_4$-SiO_2 investment materials for casting jewellery alloys. *Thermochimica Acta,* 321**,** 175-183.

JACOB, K. T., FITZNER, K. & ALCOCK, C. B. (1977) Activities in the spinel solid solution, phase equilibria and thermodynamic properties of ternary phases in the system Cu-Fe-0. *Metallurgical Transactions B,* 8**,** 451-460.

JALILEHVAND, F. (2000) Structure of Hydrated Ions and Cyanide Complexes by X-Ray Absorption Spectroscopy. *Department of Chemistry, Inorganic Chemistry.* Stockholm, Sweden, Royal Institute of Technology.

KARLFELDT FEDJE, K., EKBERG, C., SKARNEMARK, G., PIRES, E. & STEENARI, B.-M. (2012) Initial studies of the recovery of Cu from MSWI fly ash leachates using solvent extraction. *Waste Management & Research,* 30**,** 1072-1080.

KARLFELDT FEDJE, K., EKBERG, C., SKARNEMARK, G. & STEENARI, B.-M. (2010) Removal of hazardous metals from MSW fly ash - An evaluation of ash leaching methods. *Journal of Hazardous Materials,* 173**,** 310-317.

KARLSSON, S., CARLSSON, P., ÅBERG, D., KARLFELDT FEDJE, K., KROOK, J. & STEENARI, B.-M. (2010) What is required for the viability of metal recovery from municipal solid-waste incineration fly ash? - Design and assessment of a process plant for copper extraction. *Proceedings of LINNAEUS ECOTECH'10 Nov 22-24, 2010, Kalmar, Sweden.*

KOLTA, G. A. & ASKAR, M. H. (1975) Thermal decomposition of some metal sulphates. *Thermochimica Acta,* 11**,** 65-72.

LUNDHOLM, K., BOSTRÖM, D., NORDIN, A. & SHCHUKAREV, A. (2007) Fate of Cu, Cr, and As During Combustion of Impregnated Wood with and without Peat Additive. *Environmental Science & Technology,* 41**,** 6534-6540.

LUNDHOLM, K., ROGERS, J. M., HAYNES, B. S., BOSTRÖM, D. & NORDIN, A. (2008) Fate of Cu, Cr, and As during the Combustion Stages of CCA-Treated Wood Fuel Particles. *Energy & Fuels,* 22**,** 1589-1597.

MATHEWS, T., HAJRA, J. P. & JACOB, K. T. (1993) Phase relations and thermodynamic properties of condensed phases in the system calcium-copper-oxygen. *Chemistry of Materials,* 5**,** 1669-1675.

NEUMANN, J. P., ZHONG, T. & CHANG, Y. A. (1984) The Cu-O (Copper-Oxygen) system. *Bulletin of Alloy Phase Diagrams,* 5**,** 136-140.

PENNER-HAHN, J. E. (1999) X-ray absorption spectroscopy in coordination chemistry. *Coordination Chemistry Reviews,* 190-192**,** 1101-1123.

PICKUP, D. M., AHMED, I., FITZGERALD, V., MOSS, R. M., WETHERALL, K. M., KNOWLES, J. C., SMITH, M. E. & NEWPORT, R. J. (2006) X-ray absorption spectroscopy and high-energy XRD study of the local environment of copper in antibacterial copper-releasing degradable phosphate glasses. *Journal of Non-Crystalline Solids,* 352**,** 3080-3087.

RAVEL, B. & NEWVILLE, M. (2005) ATHENA, ARTEMIS, HEPHAESTUS: data analysis for X-ray absorption spectroscopy using IFEFFIT. *Journal of Synchrotron Radiation,* 12**,** 537-541.

SCHLUMBERGER, S., SCHUSTER, M., RINGMANN, S. & KORALEWSKA, R. (2007) Recovery of high purity zinc from filter ash produced during the thermal treatment of waste and inerting of residual materials. *Waste Management & Research,* 25**,** 547-555.

STANMORE, B. R. (2004) The formation of dioxins in combustion systems. *Combustion and Flame,* 136**,** 398-427.

STROUPE, J. D. (1949) An X-Ray Diffraction Study of the Copper Chromites and of the "Copper-Chromium Oxide" Catalyst. *Journal of the American Chemical Society,* 71**,** 569-572.

SUŁOWSKA, J., WACŁAWSKA, I., SZUMERA, M. & OLEJNICZAK, Z. (2012) Characterization of thermally induced of crystalline phases in CuO-containing silicate–phosphate glasses. *Journal of Thermal Analysis and Calorimetry,* 108**,** 657-663.

TAKAOKA, M., SHIONO, A., NISHIMURA, K., YAMAMOTO, T., URUGA, T., TAKEDA, N., TANAKA, T., OSHITA, K., MATSUMOTO, T. & HARADA, H. (2005a) Dynamic change of copper in fly ash during de novo synthesis of dioxins. *Environmental Science and Technology,* 39**,** 5878-5884.

TAKAOKA, M., SHIONO, A., YAMAMOTO, T., URUGA, T., TAKEDA, N., TANAKA, T., OSHITA, K., MATSUMOTO, T. & HARADA, H. (2008) Relationship between dynamic change of copper and dioxin generation in various fly ash. *Chemosphere,* 73**,** S78-S83.

TAKAOKA, M., YAMAMOTO, T., SHIONO, A., TAKEDA, N., OSHITA, K., MATSUMOTO, T. & TANAKA, T. (2005b) The effect of copper speciation on the formation of chlorinated aromatics on real municipal solid waste incinerator fly ash. *Chemosphere,* 59**,** 1497-1505.

TESSIER, A., CAMPBELL, P. G. C. & BISSON, M. (1979) Sequential extraction procedure for the speciation of particulate trace metals. *Analytical Chemistry,* 51**,** 844-851.

TIAN, S., YU, M., WANG, W., WANG, Q. & WU, Z. (2009) Investigating the Speciation of Copper in Secondary Fly Ash by X-ray Absorption Spectroscopy. *Environmental Science & Technology,* 43**,** 9084-9088.

TOLLER, S., KÄRRMAN, E., GUSTAFSSON, J. P. & MAGNUSSON, Y. (2009) Environmental assessment of incinerator residue utilisation. *Waste Management,* 29**,** 2071-2077.

TUAN, Y. J., WANG, H. P., CHANG, J. E., CHAO, C. C. & TSAIA, C. K. (2010) Speciation of copper in the thermally stabilized slag. *Nuclear Instruments and Methods in Physics Research, Section A: Accelerators, Spectrometers, Detectors and Associated Equipment,* 619**,** 316-318.

VAN HERCK, P. & VANDECASTEELE, C. (2001) Evaluation of the use of a sequential extraction procedure for the characterization and treatment of metal containing solid waste. *Waste Management,* 21**,** 685-694.

WEAST, R. C. (1975) *Handbook of Chemistry and Physics,* CRC Press.

VERHULST, D., BUEKENS, A., SPENCER, P. J. & ERIKSSON, G. (1995) Thermodynamic Behavior of Metal Chlorides and Sulfates under the Conditions of Incineration Furnaces. *Environmental Science & Technology,* 30**,** 50-56.

WIKSTRÖM, E. (1999) The Role of Chlorine during Waste Combustion. *Department of Chemistry, Environmental Chemistry.* Umeå, Sweden, Umeå University.

ZABINSKY, S., REHR, J., ANKUDINOV, A., ALBERS, R. & ELLER, M. (1995) Multiple-scattering calculations of x-ray-absorption spectra. *Physical Review B,* 52**,** 2995-3008.